International Journal of Fatigue 92 (2016) 616–622

Contents lists available at ScienceDirect

International Journal of Fatigue

journal homepage: www.elsevier.com/locate/ijfatigue

Effect of harmonic structure design with bimodal grain size distribution on near-threshold fatigue crack propagation in Ti–6Al–4V alloy

Shoichi Kikuchi [a,*], Takafumi Imai [a], Hiroki Kubozono [a], Yoshikazu Nakai [a], Mie Ota [b], Akira Ueno [b], Kei Ameyama [b]

[a] Department of Mechanical Engineering, Graduate School of Engineering, Kobe University, 1-1 Rokkodai-cho, Nada-ku, Kobe 657-8501, Japan
[b] Department of Mechanical Engineering, College of Science and Engineering, Ritsumeikan University, 1-1-1 Noji-higashi, Kusatsu, Shiga 525-8577, Japan

ARTICLE INFO

Article history:
Received 15 December 2015
Received in revised form 16 February 2016
Accepted 23 February 2016
Available online 3 March 2016

Keywords:
Fatigue
Fracture mechanics
Titanium alloy
Crack closure
Grain refinement

ABSTRACT

Titanium alloy (Ti–6Al–4V) with a bimodal harmonic structure, which consists of a coarse-grained structure surrounded by a network structure of fine equiaxed grains, has been fabricated by sintering mechanically-milled powders to achieve high strength and good plasticity. To investigate the near-threshold fatigue crack propagation in the harmonic structured Ti–6Al–4V alloy, *K*-decreasing tests are conducted on disk-shaped compact specimens (ASTM standard) under stress ratios *R* from 0.1 to 0.8 with a constant-*R* loading regime in a laboratory atmosphere. The fracture surfaces are observed using scanning electron microscopy (SEM), and crack profiles are analysed using electron backscatter diffraction (EBSD) to discuss the mechanism of the fatigue crack propagation. The crack growth rates da/dN in the harmonic structured material are constantly higher than those in a material with coarse acicular microstructure under comparable stress intensity range ΔK, while the fatigue thresholds ΔK_{th} are lower. This is attributed to a decrease in the magnitude of roughness-induced crack closure and the effective stress intensity range $\Delta K_{eff,th}$ in the harmonic structured Ti–6Al–4V alloy due to the presence of fine grains. Furthermore, in some areas, fatigue cracks do not propagate in the coarse-grained structure with higher fatigue crack growth resistance, but they preferentially propagate across the network structure of fine grains in the harmonic structure.

1. Introduction

Titanium alloy (Ti–6Al–4V) has widely been applied in various engineering fields such as biomaterials and aerospace components due to its high specific strength and excellent corrosion resistance. An improvement in the mechanical properties of titanium alloys has recently been required in the engineering fields, so that increasing the structural reliability of titanium alloy has become a very important topic. The mechanical properties of metallic materials are affected by their microstructure; therefore, the grain-refinement process is an effective approach to improve yield strength [1,2] and fatigue strength.

However, a homogeneous fine-grained structure formed by severe plastic deformation generally leads to a decrease in ductility [3–7], such as with commercially pure (CP) titanium [4,5], due to starting of their plastic instability in the early stage. Previous investigations have reported that bimodal microstructural design improves both the strength and ductility of materials [3–8]. For example, Wang et al. [6] have reported that pure copper with a bimodal grain size distribution, formed by thermomechanical treatment, exhibits stable tensile deformation, which leads to high tensile ductility. Our research group [9–17] has developed the harmonic structure, which consists of a coarse-grained structure surrounded by a network structure of fine grains. The harmonic structure is formed by sintering mechanically-milled titanium-based powders. The most significant difference between the harmonic structure and a conventional bimodal structure is that all of the fine equiaxed regions are interconnected in a continuous network. In previous studies, CP titanium [9–12] and Ti–6Al–4V alloy [12–15] with a harmonic structure exhibited high strength and high ductility compared to their homogeneous counterparts because stress and strain localization were suppressed in the harmonic structure [16]. Furthermore, it was confirmed that harmonic structured CP titanium exhibits a superior dynamic response [17].

We have focused on the fatigue properties of Ti–6Al–4V alloy with harmonic structure to achieve sufficient performance for practical applications in the engineering fields [14,15]. It has been clarified that a fatigue crack starts from the relatively

* Corresponding author. Tel.: +81 78 803 6329; fax: +81 78 803 6155.
E-mail address: kikuchi@mech.kobe-u.ac.jp (S. Kikuchi).

http://dx.doi.org/10.1016/j.ijfatigue.2016.02.038
0142-1123/

coarse-grained structure in the harmonic structure. However, the microstructure at the crack initiation site is finer than that of the material prepared from the as-received powders, which results in improved fatigue strength [14]. Another important aspect of the fatigue properties of the harmonic structured material is a near-threshold crack propagation dependent on the microstructure and stress ratio (ratio of minimum to maximum stress) [15,18–22]. In our proposed microstructure design, the grain size distribution can be controlled by changing process parameters such as the mechanical milling (MM) time [10] and the number of passes during jet milling [11]. Therefore, the effects of bimodal grain size distribution on the fatigue crack propagation in harmonic structured Ti–6Al–4V alloy should be examined.

The purpose of the present study is to examine the near-threshold fatigue crack propagation of harmonic structured Ti–6Al–4V alloy with a bimodal grain size distribution, which exhibits superior mechanical properties. Furthermore, the mechanism of fatigue crack propagation is experimentally investigated for the harmonic structured Ti–6Al–4V alloy on the basis of the crack closure concept, fractography and crystallography.

2. Experimental procedures

2.1. Material

Ti–6Al–4V alloy powder with the chemical composition shown in Table 1 is used. Fig. 1 shows a scanning electron microscopy (SEM) micrograph of the Ti–6Al–4V alloy powder. The powders (186 μm particle diameter) have been produced using the plasma rotating electrode process (PREP) [23]. The PREP can be used to fabricate spherical particles that have negligible contamination with impurities such as oxygen or nitrogen gases during the fabrication process.

Fig. 2 shows a schematic illustration of the process for the formation of the harmonic structured material with bimodal grain size distribution fabricated by MM and spark plasma sintering (SPS). MM is performed for the Ti–6Al–4V powders using a planetary ball mill (Fritch P-5) with a tungsten carbide vessel and SUJ2 steel balls in an argon gas atmosphere at room temperature, with a rotational speed of 200 rpm for 90 and 360 ks and a ball-to-powder weight ratio of 1.8:1 to create fine grains at the powder particle surfaces. The powders are subsequently consolidated by SPS at 1123 K for 1.8 ks under vacuum. The applied pressure is lower than 15 Pa and 50 MPa using a 25 mm internal diameter graphite die to produce the MM90 and MM360 materials, respectively. Sintered material fabricated from the as-received initial powders (Untreated material) and bulk material are also prepared for comparison. The MM90 material exhibits higher strength and ductility than the Untreated series [13], as is shown in Table 2. In contrast, the MM360 series shows highest strength, but lower ductility than those of Untreated series and MM90 series.

Table 1
Chemical composition of Ti–6Al–4V powder (mass%).

Al	V	Fe	H	N	O	C	Ti
6.51	4.26	0.170	0.002	0.003	0.18	0.01	Bal.

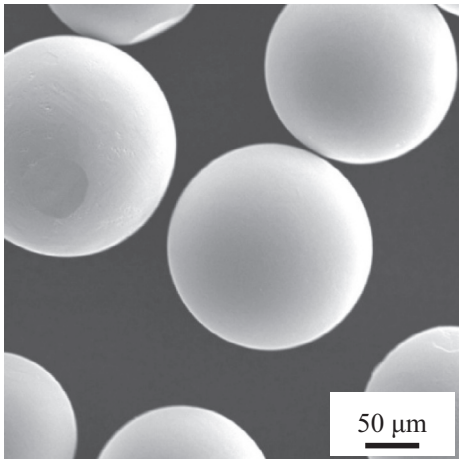

Fig. 1. SEM micrograph of Ti–6Al–4V powder.

2.2. Fatigue crack propagation test

The specimen used in the present study is the disk-shaped compact (DC(T)) specimen based on the ASTM standard. The sintered materials (7.5 mm thick, 25.2 mm diameter) are cut to approximately 2.5 mm thick and machined into the DC(T) specimen with sizes shown in Fig. 3. The specimen surfaces are then polished with emery papers (#80 to #4000) and SiO_2 suspension to obtain a mirror-finish. Two types of bulk materials are also prepared: a fine-grained bulk material (F-Bulk) and a coarse-grained material heated at 1123 K for 18 ks (C-Bulk) to examine the effect of grain size on the fatigue crack propagation of Ti–6Al–4V. Fig. 4 shows a flowchart for the specimen preparation procedure: a total of five specimen types with different microstructures are prepared.

Fatigue crack propagation tests are conducted in an electrodynamic fatigue testing machine using five different values of stress ratio R, in the range from 0.1 to 0.8. To approach the fatigue threshold, K-decreasing tests are conducted under a constant-R loading regime. Specimens are first fatigue pre-cracked for a minimum of 1 mm from the notch tip. The frequency of stress cycling is 30 Hz, and the tests are conducted in the laboratory atmosphere. The fatigue threshold ΔK_{th} is defined as the maximum value of stress intensity range under crack growth rate equal to 10^{-11} m/cycle. Crack lengths are monitored by the unloading elastic compliance method [24]. The magnitude of crack closure is also monitored; closure stress intensity K_{cl} is obtained from the closure load P_{cl}. Based on such measurements, an effective stress intensity range, $\Delta K_{eff} = K_{max} - K_{cl}$, is estimated, where K_{max} is the maximum stress intensity factor (MPa $m^{1/2}$). The value of K is calculated from the following formula (1):

$$K = Pf(\xi)/(BW^{1/2}), \quad \xi = a/W, \tag{1}$$
$$f(\xi) = (2+\xi)(0.76 + 4.8\xi - 11.58\xi^2 + 11.43\xi^3 - 4.08\xi^4)/(1-\xi)^{3/2},$$

where P is the force (N), B is the specimen thickness (m), a is the crack length (m), and W is the specimen width (m).

2.3. Microscopic observations

After crack propagation tests, the fracture surfaces and crack profiles are observed using SEM. In addition, the microstructure around the crack paths is analysed using electron backscatter diffraction (EBSD) to discuss the mechanism of fatigue crack propagation.

3. Results and discussion

3.1. Microstructural characterization of sintered materials

The microstructure of the MM series is characterized before performing the fatigue crack propagation tests. Fig. 5 shows inverse pole figure (IPF) maps and grain size color maps determined by EBSD analysis for: (a) Untreated, (b) MM90, and (c)